A Bimodal Detection-Based Tremor Suppression System for Vascular Interventional Surgery Robots

Xinming Li, *Graduate Student Member, IEEE*, Shuxiang Guo, *Fellow, IEEE*, Peng Shi, *Student Member, IEEE*, Xiaoliang Jin, *Student Member, IEEE*, Masahiko Kawanishi, and Keisuke Suzuki

***Abstract*— Vascular interventional surgery (VIS) robots generally rely on faster and more accurate signal interaction system between the master side and slave side. During actual operations, unconscious and nonlinear tremors limit the accuracy and safety for VIS robot's operation. To solve above issues, this article proposes a novel bimodal detection-based tremor suppression system to improve the accuracy of data interaction. More precisely, a bimodal tremor detection combined self-designed force sensitive resistor (FSR) and a linear encoder sensor is employed for radial and axial tremor detection, respectively. Tremor suppression method based on active restraint and passive modification is presented in this study, which can not only reduce the regular tremor but also effectively suppress the suddenly burst tremor. Experiments and performance analysis of the proposed method are evaluated from simulations and actual experimental results. Based on these evaluations, the tremor suppression method has obvious advantages for suppressing non-linear tremors and enhancing the timeliness of signal interaction, which the average computing time for tremor is 140 ms and average maximum amplitude moves to 2.47 mm. Moreover, we also discuss the issues for time delay and the transmission loss existed in actual experiments. Besides, this article has a potential impact on eliminating non-linear errors, improving the safety performance of operations for master–slave robotic system, and solving the crossing problem for time–frequency domain.**

***Index Terms*— Bimodal detection, master–slave system, nonlinear tremors, tremor suppression system, vascular interventional surgery robots.**

Manuscript received 27 April 2022; revised 20 September 2022; accepted 9 October 2022. Date of publication 21 October 2022; date of current version 3 November 2022. This work was supported in part by the Japan Society for the Promotion of Science (SPS) KAKENHI under Grant 15K2120 and in part by the National High-Tech Research and Development Program (863 Program) of China under Grant 2015AA043202. The Associate Editor coordinating the review process was Bruno Ando. *(Corresponding author: Shuxiang Guo.)*

Xinming Li, Peng Shi, Xiaoliang Jin, and Keisuke Suzuki are with the Graduate School of Engineering, Kagawa University, Takamatsu, Kagawa 761-0396, Japan (e-mail: s21d504@kagawa-u.ac.jp; s19d503@stu.kagawa-u.ac.jp; s19d505@stu.kagawa-u.ac.jp; suzuki.keisuke@kagawa-u.ac.jp).

Shuxiang Guo is with the Graduate School of Engineering, Kagawa University, Takamatsu, Kagawa 761-0396, Japan, and also with the Key Laboratory of Convergence Medical Engineering System and Healthcare Technology, Ministry of Industry and Information Technology, Beijing Institute of Technology, Haidian, Beijing 100081, China (e-mail: guo.shuxiang@kagawa-u.ac.jp).

Masahiko Kawanishi is with the Department of Neurological Surgery, Kagawa University, Takamatsu 761-0793, Japan (e-mail: mk@med.kagawa-u.ac.jp).

Digital Object Identifier 10.1109/TIM.2022.3216367

I. Introduction

RECENTLY, vascular and cardiac diseases still have a high rate of injury, disability, and death in the world. The patients will suffer various pains of strokes and heart attacks when these diseases affect their vessels and hearts. Vascular interventional surgery (VIS) is a kind of minimally invasive technology that is used to treat high-risk cardiovascular disease [1], [2]. Traditional manual surgery is also well known for obvious shortcomings the orthopedic strain injuries, long-lasting high workload, ionizing radiation damage, and high cost of training professional interventional physicians [3], [4]. Compared with traditional manual operation, tracked by using X-ray imaging to detect the position of the lesion and show the progress of operation, VIS has several remarkable advantages, including minimally invasive, painless sensation, and precision treatment [5]. Physicians generally spend a long time conducting a VIS by operating catheters and guidewires to insert into the blood vessels of a patient in an operating theater under unavoidable radiation. Hence, the emergence of VIS robots plays a virtual role in relieving the pressure of doctors, reducing X-ray radiation, increasing the coziness of patients, improving surgical stability, and operating precision [6].

Unfortunately, long surgery times, high psychological stress, and increasing age are easy to trigger the issues of hand tremors when physicians conduct cardiovascular surgery. Especially the appearance of hand tremors or burst tremors for the robot-assisted minimally invasive surgery will directly affect the accuracy of captured motion signals. Correspondingly, the safety and effectiveness of the operation will undergo a great decrease. The research of tremor suppression for master–slave robots has a potential value in the fields of eliminating operation errors and improving uneven distribution.

A. Current Related Works

During the past several years, the developments of advanced technology and science have witnessed a large number of efforts on the VIS robots [7], [8], especially for the therapy of cardiovascular diseases. For instance, the "master–slave" structure was diffusely adopted to resolve the problem of long-time X-ray radiation for interventional doctors [9]. A smart material named MR (magnetorheological) fluid was used to improve the transparency of teleoperation surgery by providing flexible and effective force feedback. The performance of transmission and movement was enhanced by experiments with a human model based on noninvasive techniques [10]. At the Beijing Institute of Technology, a novel robot-assisted system was proposed to reduce the risk of interventional surgery and improve the safety of operations [11]. Meanwhile, this kind of VIS robot has successfully finished an actual operation experiment in a famous hospital. A classification framework designed for analyzing the behaviors of physicians and recognizing the motion photographs was proposed by the Chinese Academy of Sciences for cardiovascular disease [12]. To replicate the habits of surgeons, the research group of Imperial College London came up with an integrated VIS Robotic Platform with haptic, force feedback, and navigation system [13].

Focus on the studies of tremor suppression, the team of Shanghai Jiao Tong University developed 12 degrees of freedom (DOF) to manipulate the surgical equipment and decrease operating tremors with excellent stability [14]. A new technology based on an optical fiber pressure sensor was proposed to reduce uneven distribution and offer robustness for the VIS robot [15]. Based on the method of means of support vector machine, a useful physiological tremor recognition algorithm was used to distinguish normal physiological tremor and surgical operation tremor when conducting an interventional surgery [16]. This algorithm can effectively improve the success rate of surgical operations. In addition, the recent study of Kagawa University creatively employed the viscosity change of MR fluids to provide certain resistance for the operation tremor and produce fast and precious haptic feedback for surgeons simultaneously [17]. Moreover, a supervised semi-autonomous control with multiple functions was applied for repetitive missions in a complex process of operating VIS robots [18]. The emergence of various kinds of new technologies has promoted the implementation of actual evaluation experiments in animals [19] and humans [20].

B. Challenges and Contributions

According to the part of current related work, the function and performance of existing VIS robotic systems are not ideal. Some studies have realized that the classification and identification of tremors [15] are significant for interventional surgery robots. r, the stable and complete system of tremor suppression for VIS robots has not been found so far. Especially, the process effect of burst tremor is not mentioned by previous research for a safe and accurate interventional operation. Furthermore, the VIS robots need to hold the abilities of force detection and haptic feedback within a more precise environment. Besides, the method of controlling the different viscosity to alter the haptic force for correction is extremely difficult on the master side [17]. Nonlinear error and unnatural tremors are easy to affect the precision of the entire VIS robot. These difficulties will lead to prolonged operation time, additional intraoperative risk, and disturbed doctor's diagnosis.

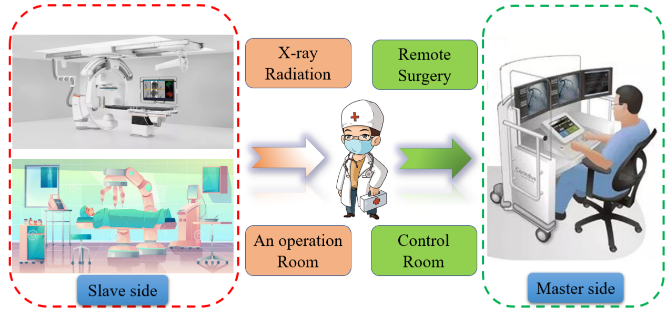

Fig. 1. Conceptual diagram of VIS robot for the surgery of cardiovascular disease.

Considering these challenges mentioned above for VIS robots, the main contribution of this study is that a bimodal detection-based tremor suppression system is proposed to detect and reduce tremors for VIS robots. A self-designed force-sensitive resistor (FSR) and a linear encoder sensor were used for radial tremor detection and axial tremor detection, respectively. Simulations and actual experiments were conducted to prove the performance of the proposed method. In addition, a unique and interesting discussion was organized according to simulation results, experiment results, and performance analysis part.

The remainder of this article is organized as follows. Section II describes the VIS robotic platform based on master–slave structure. Section III presents the details of the proposed tremor suppression system. The experiments and results are introduced in Section IV. Section V organizes the discussion for this article. At last, Section VI draws the conclusion of our study.

II. Developed Platform Description

The VIS robot for cardiovascular disease has been studied by many researchers. As shown in Fig. 1, this robot platform can be described by two core components, including the precise master device on the master side and the flexible slave manipulator on the slave side. A variety of functions for clamping the guidewire/catheter, controlling insertion and extraction of equipment, and detecting force information between the vascular surgical environment and guidewire/catheter can be provided by a slave manipulator in the VIS robot. The master device can duplicate the doctor's surgical habits by ergonomic and flexible design and offer the haptic feedback acted on the hands of operators to the take full sense of damping. The VIS robot is invented to avoid radiation, improve the safety of operation, and reduce repetitive workload for interventionalists.

A. Platform Overview

Our previous work [21] has developed an advanced tactile sensing robot-assisted system, which can reduce the burden of physicians. The developed master–slave platform of the VIS robot is shown in Fig. 2. Doctors of cardiovascular disease operate the master device in a safe and separate nonradiation room. The responsibilities of master device are providing moving and rotation data within high precision and

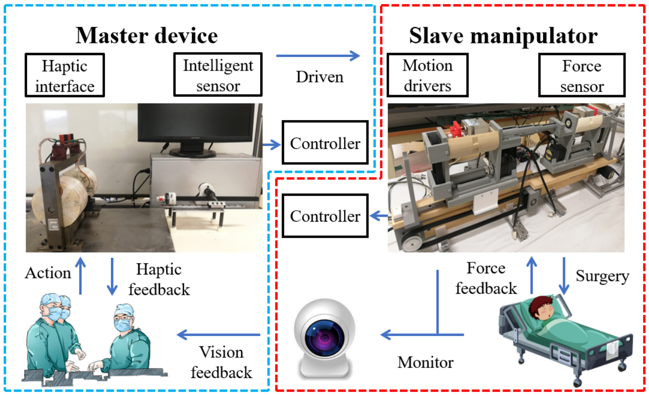

Fig. 2. Conceptual diagram of VIS robot for the robot-assisted surgery.

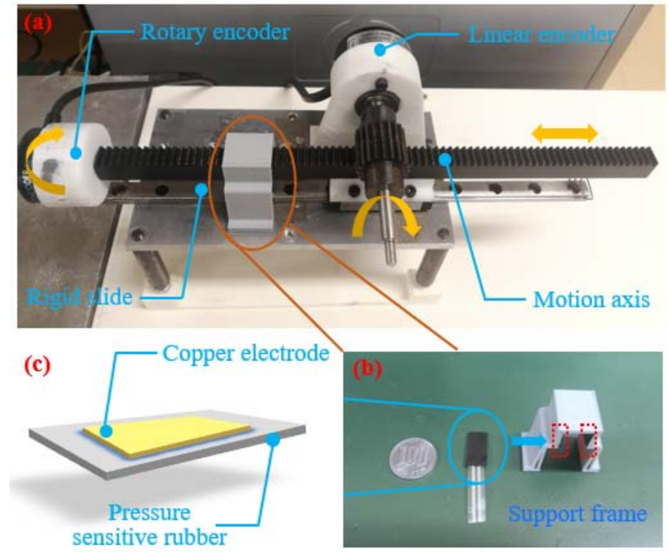

Fig. 3. Self-designed FSR based on pressure sensitive rubber. (a) Actual layout in the master device. (b) Components of the radial tremor detection. (c) Structure of FSR. (Location: The inner walls marked by red boxes.)

generating haptic feedback of the operator's hands [22]. The slave manipulator [23] duplicates the actions of a doctor to conduct a VIS operation.

Meanwhile, the position information and total proximal force of the guidewire/catheter could be fed back to the master side.

B. Master Device

A master device was invented by the previous work of our team [24]. The location of the master device is apart from the operating room, which can effectively reduce the danger of radiation exposure for surgeons. It mainly consists of two core parts named measuring unit and force feedback interface. The information on linear movement and rotational motion is collected by two intelligent encode sensors (MTL, MES020-2000P, Japan). Moreover, the master device can provide haptic feedback of the catheter's proximal force by the force feedback interface, which is based on an intelligent material, MR fluids. By changing the magnetic density of independent research magnetic fields, this interface could realize the haptic force feedback of doctors at different sensation levels.

C. Slave Manipulator

A slave manipulator is proposed in the effort [25], including a flexible catheter-driven unit and a guidewire-driven unit. Two stepping motors (ASM46AA, ORIENTAL MOTOR, Japan) are employed for flexible rotational motion and accurate retreat/advance movement. The structure of a synchronous belt can exactly enhance the precision of motion transmission. And two load cells (TU-UJ5N, TEAC, Japan) have abilities to detect the axial total force information of the catheter and guidewire simultaneously. The entire flexible invention can easily arrive at the scheduled location and collect force information at the time of conducting a surgery. This manipulator also offers a safe protection function to decrease cardiovascular disease and collision accidents between the catheter tip and the vessel wall effectively.

III. Proposed Tremor Suppression System

Tremor is a kind of unconscious jitter action generated by growing age, heavy workload, and unknown mental stress for a long surgery time. Studying tremor suppression is critical to enhancing the accuracy of radial movement and axial motion. Notably, previous effort [22] has contributed to a preliminary signal processing method and early experimental validation for tremor suppression to a certain extent. Aiming at a complete tremor suppression system with two-dimension tremors detection, this article proposed a novel tremor suppression system based on bimodal tremor detection and stacked tremor suppression method to improve the safety of operations.

A. Radial Tremor Detection

The master device is designed to make full use of the surgical experience of physicians. Besides, it has the responsibility to provide accurate motion data for the slave side. The appearance of radial hand tremors may generate unwanted disturbance signals. A self-designed FSR was used to detect the radial tremor when a doctor operated on the plastic shaft. Fig. 3 exhibits the installation location and detailed structure of the FSR. Fig. 3(a) shows the layout of FSR in the master device. The components of radial tremor detection are shown in Fig. 3(b). Moreover, Fig. 3(c) reveals the detailed structure of the FSR.

The self-designed FSR includes a support frame fabricated by three-dimensional (3-D) printed technology (ULTRABASE PRO, ANYCUBIC, China). The radial tremor model is depicted in Fig. 4 by a physical form of expression. Two pieces of FSR are used to measure the output voltage of the radial tremor. The mapping relationship between force and output voltage is calibrated by a load cell (TU-UJ5N, TEAC, Japan). Detecting radial tremors based on pressure force data captured on the master side is a novel and bold attempt for VIS robots.

B. Axial Tremor Detection

Indeed, hand tremors will be generated not only in the radial direction but also in the operation path named axial

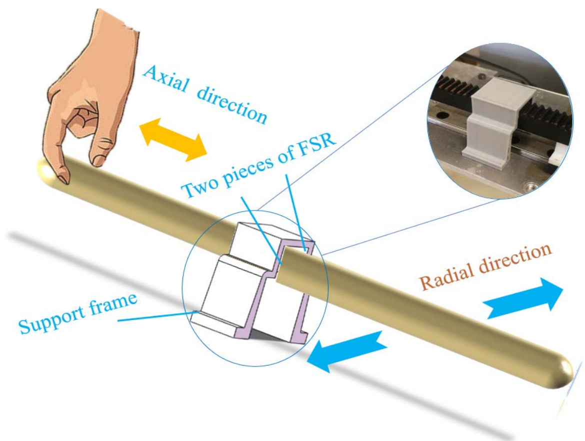

Fig. 4. Radial tremor model of physical form.

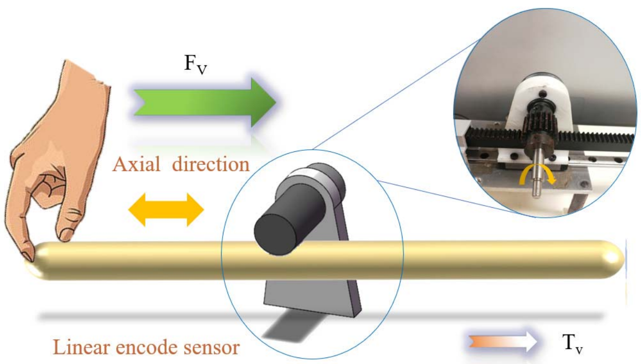

Fig. 5. Force module within axial operation tremor.

direction when a surgeon works on the master device. These unconscious tremors and physiological tremors always lead to a burst surge phenomenon for VIS robots. To reduce these tremor signals, an intelligent linear encode sensor (MTL, MES020-2000P, Japan) is employed to detect the axial tremors. Meanwhile, this sensor could provide real-time data on axial movement when operating the master device. The force module within the axial operation tremor is shown in Fig. 5.

In Fig. 5 F_v is a normal motion signal detected by a linear encode sensor. Correspondingly, a burst or a flat vibration signal is described as T_v. In addition, the actual picture of the encoder sensor is shown in the upper right of Fig. 5. Axial tremor is a common and unfriendly phenomenon during horizontal operation events. Moreover, the related parameters of tremor detection components are exhibited in Table I. It is worth mentioning that some parameter items of Table I are referred by Shi et al. [23] and Jin et al. [25]. Detailed values are determined by the size of the actual master device. Detecting and processing of axial tremors are significant in reducing the errors in moving data and improving the safety of operation.

C. Tremor Suppression Method

To address the problem of tremors in operation, a novel stacked tremor suppression method based on active restraint and passive modification is exhibited in this part. This method is adopted after detecting tremor signals by radial and axial directions. Note that vascular intervention surgery has various operational means and treatment strategies when dealing with different lesion conditions.

TABLE I
RELATED PARAMETERS OF TREMOR DETECTION COMPONENTS

Parameter items	Material	Values
Height of the support frame [25]	Polylactic Acid (PLA)	35 mm
Length of the support frame [23]	PLA	35 mm
Depth of the support frame	PLA	20 mm
Thickness the support frame	PLA	3 mm
Size of the PSR sensor	Pressure sensitive rubber	20mm×10mm
Outer diameter of the linear encoder [25]	Plastic shell	39 mm
Shaft diameter of the linear encoder [23]	Rigid metal shaft [23]	6 mm

The active restraint part is used to standardize the actions of the operators according to a priori regulation at the beginning of a surgery. In general, the band of 3–10 Hz is the common frequency of prevalent tremors of the upper limbs [26]. Tremors are not always evenly distributed in a complete signal sequence. According to [27], analysis results demonstrated two major frequency components with changeable frequency and amplitude, which contain most of the energy of the tremor signals (94.70% $\pm$ 1.40% in ET and 96.40% $\pm$ 1.39% in PT). The first part of the tremor signal is 4–6 Hz, and the second part is 8–12 Hz, that is, approximately double the frequency of the first part. Considering that the desired common tremor signals are limited between 4 and 12 Hz, the part of active restraint is used to filter unusual jitter waves during an operation. The active restraint part is the first procedure to process data collected in the master device by radial/axial tremor detection.

Active pruning function was proposed to restrain regular common hand tremors referred to in literature [28]. The surgeon's operation speed needs to be controlled in an appropriate range to improve stability and ensure safety. It is possible and dangerous that surgical equipment could puncture the blood vessel when conducting a surgery with a fast or a burst tremor. Furthermore, there will be higher risks of lumps and many sequelae for patients. The tremor signal $x(t)$ and the speed signal $v(t)$ are collected in the time domain; $f(t)$ is the corresponding frequency of tremor signal on the master side; $y(t)$ is the postpruning frequency for a tremor signal $x(t)$. Detailed equation was defined as follows:

$$y(t) = \begin{cases} \dfrac{f(t)}{12} + \theta_1[f(t) - a_2], & f(t) > a_2 \\ \dfrac{f(t)}{12}, & a_1 \leqslant f(t) \leqslant a_2 \\ \dfrac{f(t)}{12} + \theta_2[a_1 - f(t)], & f(t) < a_1 \end{cases} \tag{1}$$

where a_1 and a_2 are the lower frequency limit and the upper frequency limit, respectively, and the specific values are 4 and 12. The parameters θ_1 and θ_2 are penalty factors in $y(t)$, which are set to 0.05 and 33.56. Note that both of penalty factors are determined through multigroup experiments, and then, removing some undesirable tremor signals by a digital filter

$$x_{\mathrm{rel}}(t) = \begin{cases} x(t), & \dfrac{f(t)}{12} \leqslant \eta_0 \\ x(t) - \dfrac{x_{\max}(t) - x_{\min}(t)}{2}, & \dfrac{f(t)}{12} > \eta_0 \end{cases} \tag{2}$$

where $x_{\mathrm{rel}}(t)$ is the tremor signal after the pruning function, η_0 is the pruning threshold, which is set to 1.005. For explaining pruning (1) and (2), the underlying purpose is to trim tremors with super high frequency or too low frequency. In other words, pruning some undesirable tremors that are not within a limited frequency range (4–12 Hz). By the action of penalty factors, all of the pruning frequencies of tremors $y(t)$ would be resigned a value based on the parameter $f(t)/12$. After the process of digital filter, unsatisfactory tremor signals with super high frequency or too low frequency will be effectively pruned. At this point, the active restraint part finishes its trimming function.

The passive modification part is employed to achieve the goal of further corrections as the second part of tremor suppression method. Supposing a desired situation arises without any tremor when a surgery is conducted, the normal tremor signal can usually be approximated as a cosine curve. F_n represents the amplitude of normal motion within harmonic form. Hence, the motion signal F_{v0} can be shown as

$$F_{v0} = F_n \cos \omega t \tag{3}$$

where ω is parameter of the corresponding frequency. T_v and F_v have been introduced in Section III-B. Based on the force model, motion signal could be described as

$$F_v = F_n \cos \omega t (1 + \cos \theta) \tag{4}$$

where θ is offset angle of the axial direction. The actual horizontal motion signal includes normal linear motion signals and regular, burst, and hybrid occasional tremor signals. A novel hybrid filtering strategy was proposed to accomplish the goal of further correction. Three kinds of filters would be stacked to act on the motion signals sampled in the master device, which are processed after the course of active restraint.

First, the median average filter is adopted to obtain tremor signals with less abnormal data. Processing steps include sampling N data, wiping off the minimum value, and the maximum value in this consequent queue. An average sample signal S_a, which is a more precise median value in a sampling queue, could be gained by computing arithmetic average of $N - 2$ maintain data. In general, common value of N is a positive integer during the interval of 5–14. The maximum allowable deviation S_0 of sampling with an absolute value is determined between the average sample signal S_a and repetitive experiments. S_t is the tremor signal. Abnormal data is removed by the following equation:

$$S(t) = \begin{cases} S(t) & |S(t) - S_a| \leqslant S_0 \\ \text{Remove} & |S(t) - S_a| > S_0. \end{cases} \tag{5}$$

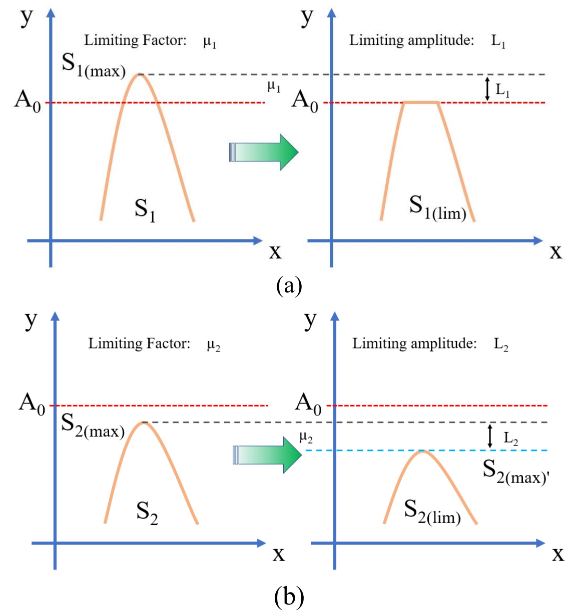

Fig. 6. Mathematical signal models of amplitude limiter filter. (a) Amplitude limiter process for burst/hybrid tremor. (b) Amplitude limiter process for regular tremor.

Second, limiting the amplitude of the tremor signals by the amplitude limiter filter. The greatest advantage of this kind of filter is reducing the signal interference caused by accidental factors. Fig. 6 depicts the mathematical signal models of the amplitude limiter filter for burst/hybrid tremor and regular tremor, respectively. A_0 is a division amplitude for distinguishing burst tremor and regular tremor, which is acquired by experiments; μ_1 and μ_2 are the limiting factors, L_1 and L_2 are the limiting amplitude, $S_{1(\max)}$ and $S_{2(\max)}$ are the maximum original amplitudes, $S_{2(\mathrm{lim})}$ represents a limited signal for regular tremor S_2, $S_{2(\max)'}$ and is maximum amplitude for the limited signal $S_{2(\mathrm{lim})}$

$$\begin{cases} A_0 = S_{1(\max)} \times (1 - \mu_1) \\ L_1 = S_{1(\max)} - A_0, \end{cases} \quad S_{1(\max)} > A_0 \tag{6}$$

$$\begin{cases} S_{2(\mathrm{lim})} = S_2 \times (1 - \mu_2) \\ L_2 = S_{2(\max)} - S_{2(\max)'}, \end{cases} \quad S_{2(\max)} \leqslant A_0. \tag{7}$$

Third, the exponential smoothing filter takes advantage of smoothing signals as the final step for tremor suppression with burst operation signals. The most insignificant merit of the exponential smoothing filter is that the weight of the motion signal exponentially decays with a fixed weight ω_0 over time. The amplitude will be corrected with the growth of time according to (8) for burst/hybrid tremor and (9) for regular tremor

$$A_{0(t_2)} = (1 - \omega_0) \times A_{0(t_1 - 1)} + C_1(t_1), \quad t_1 \in \{1, 2, 3 \ldots N, N+1\} \tag{8}$$

$$S_{2(t_2)} = (1 - \omega_0) \times S_{2(t_2 - 1)} + C_2(t_2), \quad t_2 \in \{1, 2, 3 \ldots N, N+1\} \tag{9}$$

where ω_0 is the decay weight with a value of 0.003, and $A_{0(t_1)}$ means the predictive amplitude value in a forward sequence;

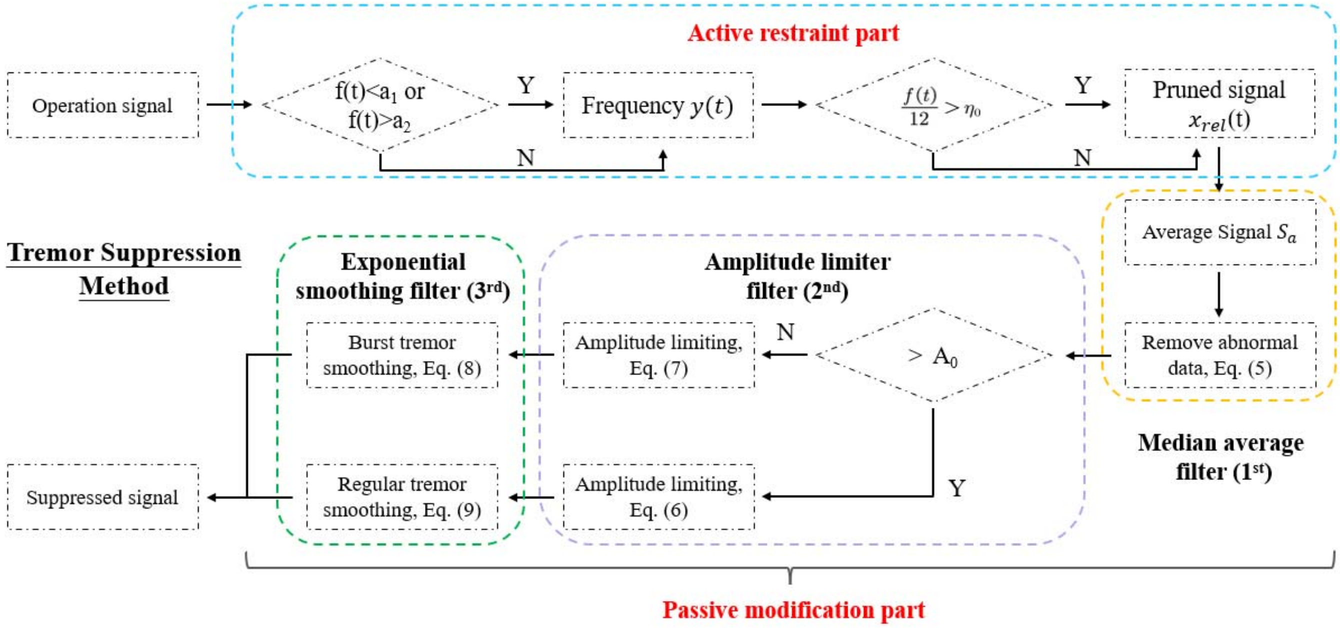

Fig. 7. Flowchart of suppression mechanism for proposed tremor suppression method.

t_1 and t_2 are the numbers of tremor subjects, and $S_2(t_2)$ is the regular tremor signal with the number t_2. The value of correction coefficients treated by amplitude limiter filter are represented as $C_1(t_1)$ and $C_2(t_2)$. Especially, a smoother and flatter signal would be embraced when detected signals have burst fluctuations under the actual operating environment. Meanwhile, the exponential smoothing filter is able to reduce computing time for tremor processing based on the merit of a fixed weight.

The detailed processing for the suppression mechanism is presented by a flowchart, which is shown in Fig. 7. The framework of the proposed tremor suppression system has been shown in Fig. 8. The correlation is built between the master–slave robot and the proposed tremor suppression system. This hybrid filtering method mixes with various advantages of different filters to reduce the unexpected tremors generated in operations. The accuracy of moving data can be improved, and tremor signals with larger amplitude and higher frequency will be suppressed by this method.

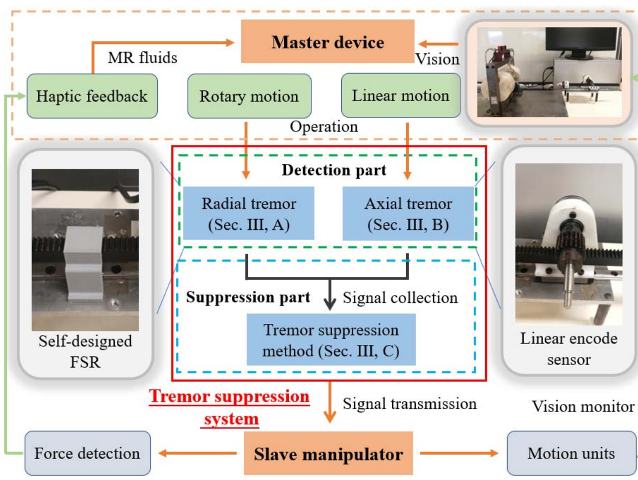

Fig. 8. Framework of proposed tremor suppression system.

IV. Experiments and Results

In this section, MATLAB simulations and glass vascular model intervention experiments have been conducted to verify the performance of this proposed tremor suppression system; simulation results can qualitatively exhibit the feasibility of the tremor suppression method. Furthermore, the real scale glass model vascular experiments can show the performance directly. At last, the performance analysis part is presented to evaluate the details of dealing with tremors in operation.

A. Simulation Results

Considering vibrations of mechanical structures and tremors of human hands during the process of operation. The detected moving data always generates different levels of interference. The moving signals with tremors will affect the amplitude and the accuracy of actual collection data. In this section, the linear motion signal without tremor is known as the desired line with a specific slope. Regular tremor represents a kind of uniform operating cosine signal that exists in practice. Burst tremor is also a cosine signal with twice the amplitude of a regular tremor. Moreover, the hybrid tremor is a combination signal of a regular tremor and a burst tremor. We set the operating speed of the master device at 3 mm/s, which is shown as the line without a tremor in Fig. 9. With the aim of simulating and operating a regular tremor, a cosine signal with a frequency of 5 Hz and amplitude of 2 mm is adopted as the regular tremor. Another cosine signal with a frequency of 5 Hz and amplitude of 4 mm is used to provide a burst tremor in this simulation experiment. The details of the simulation results of the proposed method are given in Fig. 9.

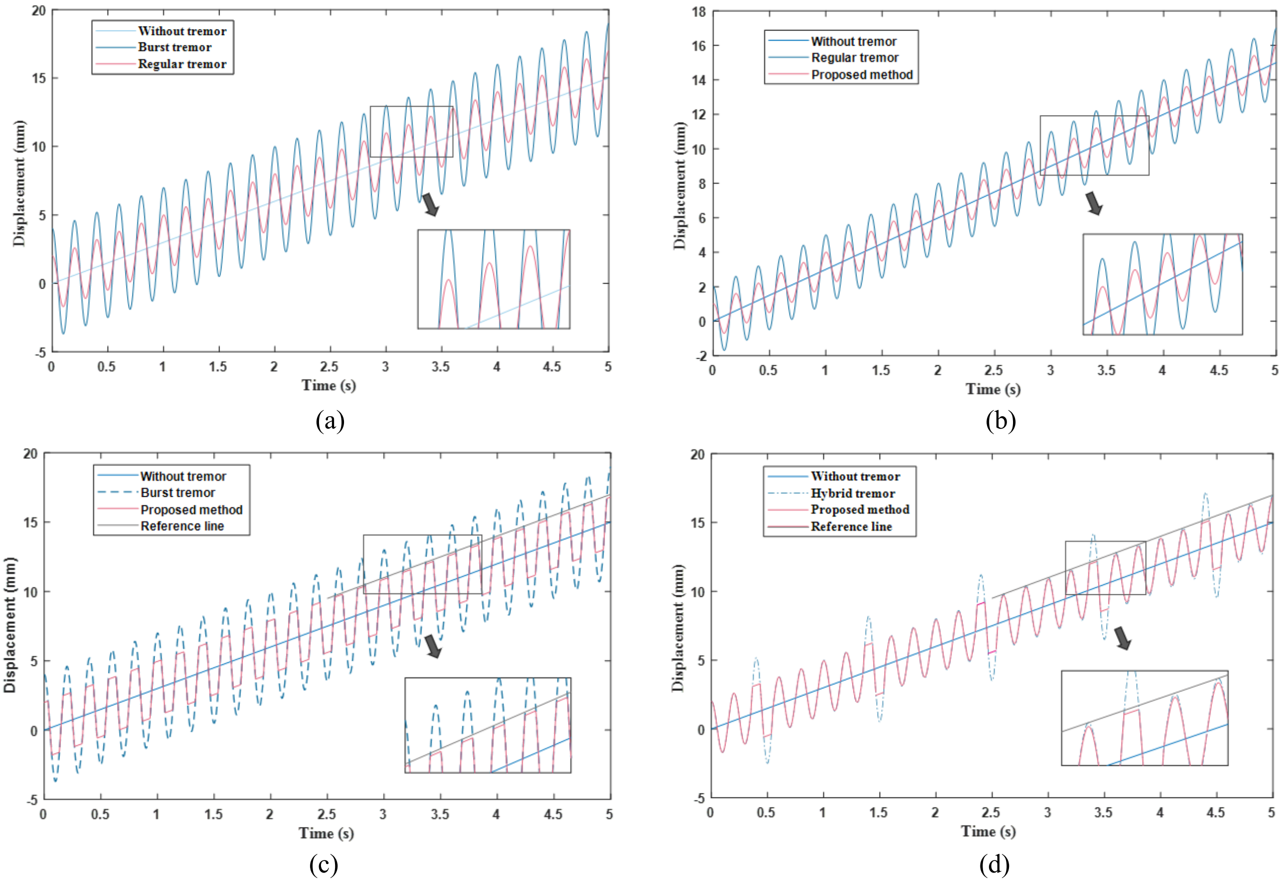

Fig. 9. Results of simulation. (a) Simulation signal without tremor, with burst tremor, and regular tremor. (b) Result for regular tremor with the proposed method. (c) Result for burst tremor with the proposed method. (d) Result for hybrid tremor with the proposed method.

From Fig. 9(b), it is seen that regular tremor is undergoing an intuitive amplitude reduction with a value of 1 mm by the proposed method. As shown in Fig. 9(c), the proposed method can deal with burst tremor based on fixed ω_0. The reduction value is getting gradually increased, which can show the variance between the reference line and tremors of the red curve. In addition, the hybrid signal can be reduced by the proposed method, which is shown in Fig. 9(d). The hybrid tremors conclude regular tremors and burst tremors simultaneously. Above all, the proposed method has a good performance in dealing with regular, burst, and hybrid tremors from this simulation part.

It is necessary to briefly discuss the simulation results. The proposed method has the ability to directly reduce amplitudes of regular and burst tremors by filters, which means the moving signal measured in the master device will embrace a more accurate value. Moreover, for the hybrid tremor, the signal curve after processing can be divided into two types, burst part and regular part. Several burst signals are reassigned by a small value. Regular signals are reduced based on a fixed decay weight ω_0 with a value of 0.003. Hence, the processed curve has a gradual tendency to deviate from the reference line. The actually acquired motion signals on the master side are, however, not as normal and regular as the simulated curves. It is significant to test the effect by insertion experiments.

B. Experimental Results

In order to test the performance of the proposed tremor suppression system in endovascular interventional robotic condition, in vitro experiments are proposed in this section. At the beginning, radial tremors are detected by FSR. Aiming at the requirements of I/O ports, controllability, fast response for transmission, communication approach, integrated data acquisition, and process, and the controller of this system are chosen by "Arduino Mega 2560," which has obvious advantages for satisfying laboratory needs. The controller serves three roles, including collecting operation data, suppressing tremor signals, and transmitting data to the slave side. By recording the voltages of FSR in different moments, the details of the corresponding force message can be calibrated by multiple experiments. Fig. 10 reveals the voltages detected by FSR and calculated force data at the same time. The conductance of FSR varies in different moments, which is a changed value due to the nonlinear characteristic of resistance. The corresponding value of force as a sudden signal is under the degree of 1 N, which is displayed in Fig. 10. In the recording of voltage readings, the value is maintained at 3.0–4.5 V when the tremors happen in radial orientation.

As another important moving information, the axial tremors are collected by the linear encoder. The details of horizontal motion are depicted in Fig. 11. The linear encoder records data

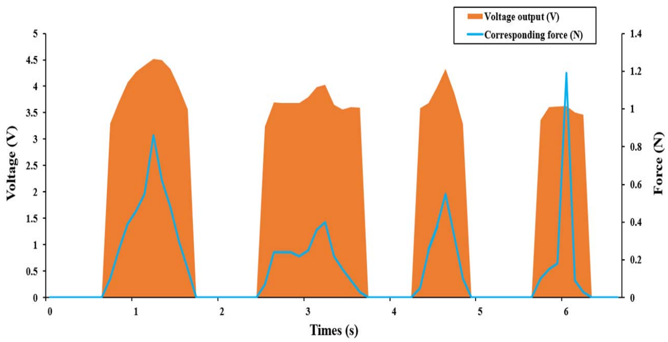

Fig. 10. Voltage output of FSR and corresponding value of force for radial tremor detection.

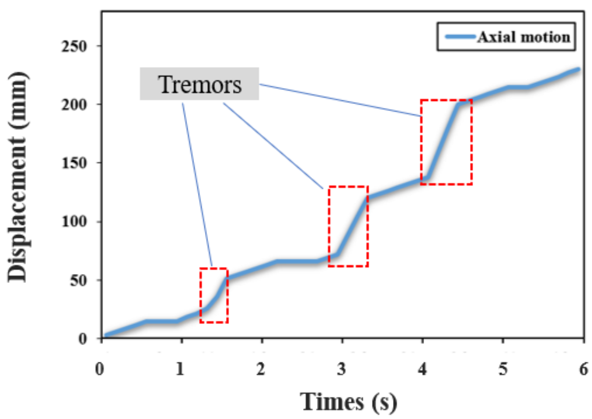

Fig. 11. Tremor detection results for axial encode sensor.

by counting the number of rotation angle pulses. The gradient of different positions represents different operation speeds. Hence, the tremor signals are always with burst gradients, which are marked by red boxes. The signal of flat gradient depicts the motion with constant velocity.

Then, the actual experiments on the slave side are alternately conducted with or without the proposed method for VIS by comparing the position information arrived through the tip of the guidewire/catheter and proximal force information captured by the load cell to certify the performance of the proposed system. First, recording the initial area of the equipment tip when doctors operate the master device under a natural regular tremor. Second, the operator suddenly provides an appropriate burst tremor, which is a detectable signal by his hands. Finally, using an intelligent network camera (VIV-TEK, USA) to monitor the actual position of the guidewire/catheter within the tremor suppression system. The experiment environment setup is shown in Fig. 12. It is noted that all experiments in this part need to hold a safe operational behavior under a gentle frequency and speed. At the same time, the blood vessel model needs to be humidified before the experiments. The actual experimental results are exhibited in Fig. 13. Blue line and orange line represent the displacement of the guidewire/catheter's tip with or without the proposed method. The average reduction of displacement is 11.26 mm. From Fig. 13, although the processing signal has some small uneven delays with different degrees. The amplitude of motion has been effectively reduced, which means the safety and accuracy of operations have obvious improvement by the proposed tremor suppression system. In addition, the force of the guidewire with actual tremors and the force of the guidewire by the proposed method is displayed in Fig. 14, which are colored with blue and orange lines. The maximum value for the force of the guidewire with actual tremors is 1.84 N, and the maximum value for the force of the guidewire by the proposed method is 1.51 N. It is clear to say that the proposed method has advantages in tremor reduction and safe operation.

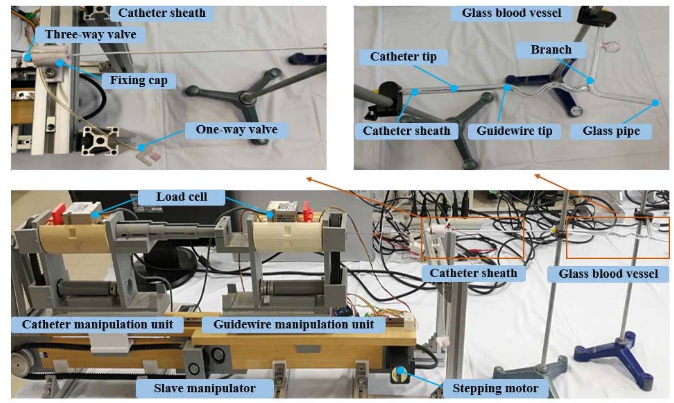

Fig. 12. Experimental setup for glass blood vessel.

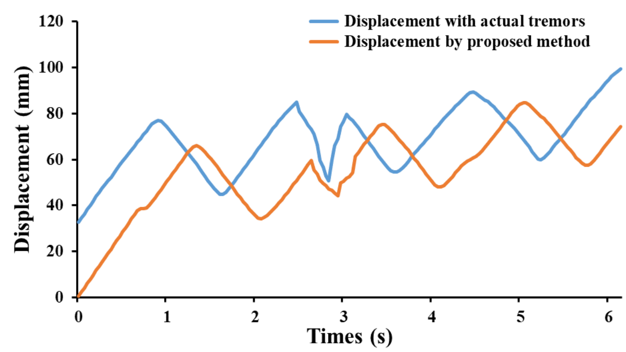

Fig. 13. Comparison displacement results for tremor suppression with the proposed method.

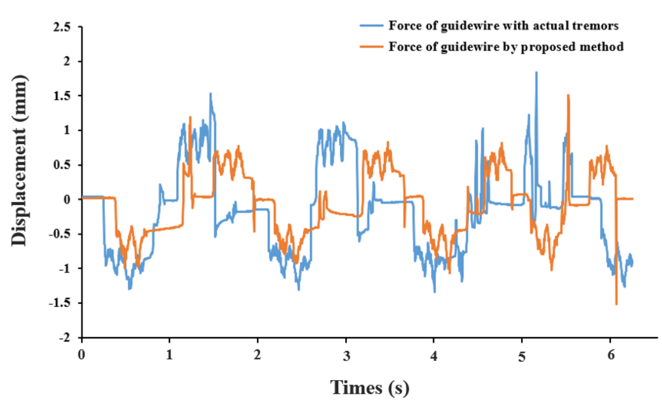

Fig. 14. Comparison force results with actual tremors and processed by the proposed method.

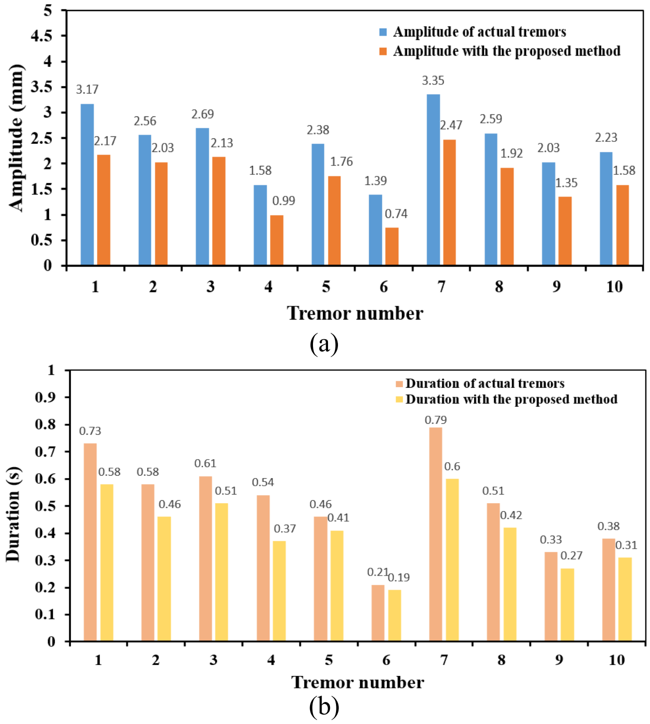

Fig. 15. Comparison qualitative analysis of ten different tremors. (a) Amplitude performance with the proposed method or not. (b) Duration performance with the proposed method or not.

C. Performance Analysis

The experiments for the proposed method have been conducted in previous sections. In this section, the tremor suppression rate (TSR) is employed in this study, which can reflect the error and the effect of tremor suppression. The index of TSR (TRE in [17]) is defined as follows:

$$\mathrm{TSR} = 1 - \frac{A_{\mathrm{pro}}}{A_{\mathrm{act}}} \tag{10}$$

where is the amplitude of tremor with actual tremors, and means the amplitude of moving position processed by the proposed method in experiments of the glass blood vessel. Under an experimental sequence, we recorded the data of ten tremor occurrences. The amplitude and the duration of different tremors were counted with the proposed tremor suppression method or not, which are shown in Fig. 15. Across all the data of ten subjects, the average maximum amplitude and average minimum amplitude of actual tremors are 3.35 and 1.39 mm. And the process of the proposed method, these two indexes move to 2.47 and 0.74 mm. Meanwhile, the value of average duration of subjects changes to 0.412 s from the original 0.514 s, which can be seen in Fig. 15(b). The proposed method has better effects on reducing amplitude and shortening duration at the same time.

In addition, the indexes of running time and the TSR performance are computed to test the further performance in this section. The timeliness performance is represented by the running time when the proposed method processed each subject. The TSR performance [17] indicates the degree of suppression based on (7). It is critical to highlight that the running time can also represent the superiority of the proposed method during the process of dealing with different tremors, which can enhance the safety and transparency of a VIS operation. The detailed comparison results of running time and TSR are shown in Fig. 16. From the obvious comparison results, all of the running times of ten subjects are below 300 ms, and the average computing time is 140 ms. The value of TSR has a clear interval from 0.2 to 0.5 (percentage is 20%–50%), which reflects the performance of solving different tremors during operations.

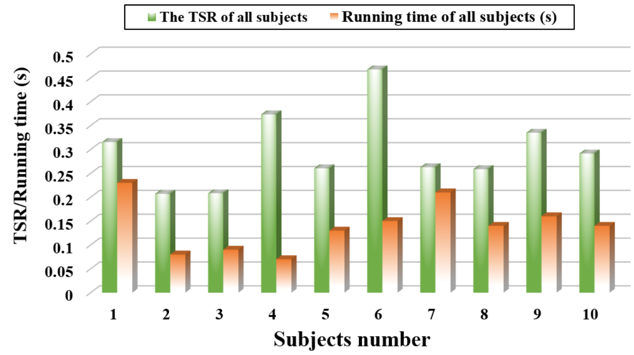

Fig. 16. Comparison results of the running time and TSR of ten subjects.

Moreover, although the proposed method has problems of uncertain time delay and very little transmissions packet loss, the regular tremors and burst tremors can be effectively reduced to a certain extent. In addition, the proposed method also has potential benefits for shortening surgery time, improving operational safety, and the making robot-assisted environment better.

V. Discussion

For the sake of resolving challenges [29] described in Section I, this article designed a bimodal detection-based tremor suppression system for VIS robots. The system has the potential values to suppress tremors and weaken nonlinear interferences during the operations of master–slave robots. A performance comparison between the proposed system and existing suppression techniques for VIS is shown in Table II, including four types of methods. Omega 3 [8] is a robot arm with excellent tracking performance designed by a commercial company. Unfortunately, the specific work for tremor suppression cannot be found. Wang et al. [14] proposed a 12 DOFs robot to reduce surgical tremors, which is a structural solution with drawbacks of high consumption and huge volume. Besides, it is an attempt at tremor suppression by changing the viscosity of MR fluids [17]. However, the control for altering viscosity is exactly hard and nonlinear in the actual experimental environment.

In Table II, the performance indexes consist of tracking error (see [25]), TSR, and Identification range of the force (IRF, see [7]). Tracking error represents the tracking performance of different VIS robots between the master side and the slave side, which is detected by distance-measuring sensors. The TSR has the same formula as tremor elimination rate (TRE) refer to literature [17], is defined in (10), which indicates the degree of suppression performance. IRF is detected by

TABLE II
PERFORMANCE COMPARISON FOR PROPOSED TREMOR SUPPRESSION SYSTEM AND OTHER STUDIES

Relevant efforts	Realization	Tremor processing	Usage (LD/ CD)	Performance		
				Tracking error (mm)	TSR	IRF (N)
Proposed tremor suppression system, 2022	FSR, encoder & method	Detection & suppression	LD	< 1.57 mm	TSR: 20%-50%	< 1.51 N
Omega 3 & SMN [8], 2018	Robot arm	No	CD	< 0.01 mm [7]	Not mentioned	Not clear
Multi-manipulators [14], 2018	12 DOFs robot	Mechanical design	LD	< 0.48 mm	Not mentioned	< 12.5 N
A tremor reduction method [17], 2021	MR fluids damper	Viscosity alteration	LD	Not mentioned	TRE [17]: 92.82%-99.45%	Not clear

- FSR: Force Sensitive Resistor
- SMN: Slave Manipulator
- CD: Commercial Device
- MR: Magnetorheological
- DOF: Degrees of Freedom
- LD: Laboratory Design
- TSR: Tremor Suppression Rate
- TRE: Tremor Elimination Rate (Same formula with TSR)
- IRF: Identification Range of the Force [7]

a force sensor located on the slave side, which represents the performance of safe operating in robot-assisted surgery. It is noted that these performance data are obtained from corresponding references. The performance parameters of the proposed system are detected by the sensors mound on the slave side and calculated by computer. Although these relevant efforts for tremor suppression are not calculated or detected by a completely similar condition, Table II can indicate that the proposed tremor suppression method shows good behavior by the performance of tracking error, TSR, and IRF. Compared to the effort [8] and effort [14], the proposed system is well performed in IRF ($<$1.51 N), which means the robotic system will embrace a safer operating environment for VIS. As for the index of tracking error, despite the data of the proposed system being a little bit larger than commercial arm robot [8] and multimanipulators design [14], it is still safe. (The VIS system is considered safe if the tracking error is less than 2 mm [7].) Based on the TSR performance, the proposed system (20%–50%) has a positive influence compared to the TRE in [17]. In addition, the IRF is not mentioned in the effort [17], and so our suppression system also has advantages compared to the effort [17]. Moreover, we compared the realization, tremor processing, and usage ways with relevant efforts, which is clear to see that the proposed system is a complete solution for tremor detection and suppression in the laboratory environment. Above all, it is believed that the proposed tremor system is well performed for robot-assisted surgery.

According to the simulation results, the experiments showed better performances in reducing burst tremors and decreasing regular tremors simultaneously (see Fig. 9) with the average running time below 100 ms. Unfortunately, the results for hybrid tremors have risks of decreasing signal due to the exponential smoothing filter within a lesser decay rate. Although the data weakening problem exists [30], the proposed method still enables nonlinear interference and regular tremor to embrace a good suppression effect according to performance analysis. From the experimental results, the bimodal detection used by self-designed FSR and linear encoder sensor shows a good display in detecting tremors (see Figs. 10 and 11). Furthermore, we creatively try to reduce tremors based on a combination of the time domain and frequency domain [see (1)]. The better performance in actual in vitro experiments is proven by the comparison displacement results (see Fig. 13) and comparison force results (see Fig. 14). By the performance analysis of ten subjects, the comparative amplitude and duration information (see Fig. 15) reveals that the proposed method is capable of suppressing the amplitude and shortening the duration when tremors appear. In addition, the timeliness performance (running time) and TSR performance of the proposed method also indicate that the proposed tremor suppression system has good abilities for reducing amplitude and shortening duration when tremor occurs (see Fig. 16). The issues of processing delay and transmission loss, however, still exist during the actual experiments (see Fig. 13). Some advance control algorithms [31], excellent data transmission technology [32], high-precision sensors [33], and real-time detection systems [34] may have abilities to react to these problems [35] in the near future.

VI. CONCLUSION

In this article, a tremor suppression system was presented to enhance the security and accuracy in the robotic vascular interventional procedure. First, the radial tremor detection and axial tremor detection was adopted to monitor the occurrence of tremors in a multimodality manner. Second, a tremor suppression method based on active restraint and passive modification was proposed for the suppression of burst and regular tremors. Finally, simulation results and actual experiment results can both illustrate that the proposed method has obvious advantages for suppressing nonlinear tremors and improving the timeliness of signal processing. According to the performance analysis, it is clear that some potential benefits for improving operational safety and reducing surgery time in the proposed tremor suppression system.

In the future, more advance-technology and high-precision detection equipment would be used in VIS robots to capture more accurate motion data. And if possible, the proposed system will be verified through animal or even human experiments.

REFERENCES

[1] V. Sitaramgupta, T. Sakorikar, and H. J. Pandya, "An MEMS-based force sensor: Packaging and proprioceptive force recognition through vibro-haptic feedback for catheters," *IEEE Trans. Instrum. Meas.*, vol. 71, pp. 1–11, 2022, doi: 10.1109/TIM.2022.3141168.

[2] X. Yin, C. Wu, S. Wen, and J. Zhang, "Smart design of Z-width expanded thumb haptic interface using magnetorheological fluids," *IEEE Trans. Instrum. Meas.*, vol. 70, pp. 1–11, 2021, doi: 10.1109/TIM.2021.3112231.

[3] M. G. Andreassi, E. Piccaluga, G. Guagliumi, M. Del Greco, F. Gaita, and E. Picano, "Occupational health risks in cardiac catheterization laboratory workers," *Circulation, Cardiovascular Interventions*, vol. 9, no. 4, Apr. 2016, Art. no. e003273.

[4] L. W. Klein and E. P. Campos, "Occupational hazards in the cath lab—Physician, protect thyself!" *J. Invasive Cardiology*, vol. 30, no. 2, pp. 75–76, 2018.

[5] X. Jin, S. Guo, J. Guo, P. Shi, M. Kawanishi, and H. Hirata, "Active suppression method of dangerous behaviors for robot-assisted vascular interventional surgery," *IEEE Trans. Instrum. Meas.*, vol. 71, pp. 1–9, 2022, doi: 10.1109/TIM.2022.3170997.

[6] J. Guo, X. Jin, S. Guo, and Q. Fu, "A vascular interventional surgical robotic system based on force-visual feedback," *IEEE Sensors J.*, vol. 19, no. 23, pp. 11081–11089, Dec. 2019.

[7] W. Zhou, S. Guo, J. Guo, F. Meng, Z. Chen, and C. Lyu, "A surgeon's habits-based novel master manipulator for the vascular interventional surgical master-slave robotic system," *IEEE Sensors J.*, vol. 22, no. 10, pp. 9922–9931, May 2022.

[8] H. Shen, C. Wang, L. Xie, S. Zhou, L. Gu, and H. Xie, "A novel remote-controlled robotic system for cerebrovascular intervention," *Int. J. Med. Robot. Comput. Assist. Surgery*, vol. 14, no. 6, p. e1943, Dec. 2018.

[9] X. Yin, S. Guo, N. Xiao, T. Tamiya, H. Hirata, and H. Ishihara, "Safety operation consciousness realization of a MR fluids-based novel haptic interface for teleoperated catheter minimally invasive neurosurgery," *IEEE/ASME Trans. Mechatronics*, vol. 21, no. 2, pp. 1043–1054, Apr. 2016.

[10] S. Guo, Y. Song, and X. Yin, "A novel robot-assisted endovascular catheterization system with haptic force feedback," *IEEE Trans. Robot*, vol. 35, pp. 685–696, Mar. 2019.

[11] X. Bao, S. Guo, and N. Xiao, "Compensatory force measurement and multimodal force feedback for remote-controlled vascular interventional robot," *Biomed. Microdevice*, vol. 20, no. 3, p. 74, Aug. 2018.

[12] X.-H. Zhou, G.-B. Bian, X.-L. Xie, Z.-G. Hou, R.-Q. Li, and Y.-J. Zhou, "Qualitative and quantitative assessment of technical skills in percutaneous coronary intervention: In Vivo porcine studies," *IEEE Trans. Biomed. Eng.*, vol. 67, no. 2, pp. 353–364, Feb. 2020.

[13] M. E. M. K. Abdelaziz et al., "Toward a versatile robotic platform for fluoroscopy and MRI-guided endovascular interventions: A pre-clinical study," in *Proc. IEEE/RSJ Int. Conf. Intell. Robots Syst. (IROS)*, Nov. 2019, pp. 5411–5418.

[14] K. Wang et al., "Endovascular intervention robot with multi-manipulators for surgical procedures: Dexterity, adaptability, and practicability," *Robot. Comput.-Integr. Manuf.*, vol. 56, pp. 75–84, Apr. 2019.

[15] T. O. Akinyemi et al., "Fiber Bragg grating-based force sensing in robot-assisted cardiac interventions: A review," *IEEE Sensors J.*, vol. 21, no. 9, pp. 10317–10331, May 2021.

[16] S. Guo, L. Zhang, C. Yang, and R. Shen, "Recognition and filtering of tremor signals for vascular interventional surgical robot," in *Proc. IEEE Int. Conf. Mechatronics Autom. (ICMA)*, Oct. 2020, pp. 1642–1646.

[17] L. Zheng and S. Guo, "A magnetorheological fluid-based tremor reduction method for robot assisted catheter operating system," *Int. J. Mechtron. Autom.*, vol. 8, no. 2, pp. 72–79, 2020.

[18] J. Chen et al., "Supervised semi-autonomous control for surgical robot based on banoian optimization," in *Proc. IEEE/RSJ Int. Conf. Intell. Robots Syst. (IROS)*, Oct. 2020, pp. 2943–2949.

[19] A. Azizi, C. C. Tremblay, K. Gagné, and S. Martel, "Using the fringe field of a clinical MRI scanner enables robotic navigation of tethered instruments in deeper vascular regions," *Sci. Robot.*, vol. 4, no. 36, Nov. 2019.

[20] X. Bao et al., "Operation evaluation in-human of a novel remote-controlled vascular interventional robot," *Biomed. Microdevices*, vol. 20, no. 2, p. 34, Jun. 2018.

[21] X. Jin et al., "Total force analysis and safety enhancing for operating both guidewire and catheter in endovascular surgery," *IEEE Sensors J.*, vol. 21, no. 20, pp. 22499–22509, Oct. 2021.

[22] X. Li, S. Guo, P. Shi, and X. Jin, "A novel tremor suppression method for endovascular interventional robotic systems," in *Proc. IEEE Int. Conf. Mechatronics Autom. (ICMA)*, Aug. 2021, pp. 1050–1054.

[23] P. Shi et al., "Design and evaluation of a haptic robot-assisted catheter operating system with collision protection function," *IEEE Sensors J.*, vol. 21, no. 18, pp. 20807–20816, Sep. 2021.

[24] L. Zhang et al., "Design and performance evaluation of collision protection-based safety operation for a haptic robot-assisted catheter operating system," *Biomed. Microdevices*, vol. 20, no. 2, p. 22, 2018.

[25] X. Jin, S. Guo, J. Guo, P. Shi, T. Tamiya, and H. Hirata, "Development of a tactile sensing robot-assisted system for vascular interventional surgery," *IEEE Sensors J.*, vol. 21, no. 10, pp. 12284–12294, May 2021.

[26] A. H. Zamanian and E. Richer, "Adaptive notch filter for pathological tremor suppression using permanent magnet linear motor," *Mechatronics*, vol. 63, Nov. 2019, Art. no. 102273.

[27] B. Taheri, D. Case, and E. Richer, "Adaptive suppression of severe pathological tremor by torque estimation method," *IEEE/ASME Trans. Mechatronics*, vol. 20, no. 2, pp. 717–727, Apr. 2015.

[28] X.-C. Yin, X. Yin, K. Huang, and H.-W. Hao, "Robust text detection in natural scene images," *IEEE Trans. Pattern Anal. Mach. Intell.*, vol. 36, no. 5, pp. 970–983, May 2014.

[29] L. Zheng, S. Guo, and L. Zhang, "Preliminarily design and evaluation of tremor reduction based on magnetorheological damper for catheter minimally invasive surgery," in *Proc. IEEE Int. Conf. Mechatronics Autom. (ICMA)*, Aug. 2019, pp. 2223–2229.

[30] Y. Song et al., "Performance evaluation of a robot-assisted catheter operating system with haptic feedback," *Biomed. Microdevices*, vol. 20, no. 2, p. 50, Jun. 2018.

[31] C. R. Kelley and J. L. Kauffman, "Tremor-active controller for dielectric elastomer-based pathological tremor suppression," *IEEE/ASME Trans. Mechatronics*, vol. 25, no. 2, pp. 1143–1148, Apr. 2020.

[32] Y. Zhou, M. E. Jenkins, M. D. Naish, and A. L. Trejos, "Design and validation of a novel mechatronic transmission system for a wearable tremor suppression device," *Robot. Auton. Syst.*, vol. 91, pp. 38–48, May 2017.

[33] H. Zang, X. Zhang, H. Zhang, B. Zhu, and S. Fatikow, "A novel force sensor based on optical fibers used for semicircular flexure beam unit," *IEEE Trans. Instrum. Meas.*, vol. 71, pp. 1–10, 2022, doi: 10.1109/TIM.2021.3134308.

[34] X. Li, S. Guo, P. Shi, X. Jin, and M. Kawanishi, "An endovascular catheterization robotic system using collaborative operation with magnetically controlled haptic force feedback," *Micromachines*, vol. 13, no. 4, p. 505, Mar. 2022.

[35] A. Zahedi, B. Zhang, A. Yi, and D. Zhang, "A soft exoskeleton for tremor suppression equipped with flexible semiactive actuator," *Soft Robot.*, vol. 8, no. 4, pp. 432–447, Aug. 2021.

Xinming Li (Graduate Student Member, IEEE) received the M.S. degree from the Tianjin University of Technology, Tianjin, China, in 2020. He is currently pursuing the Ph.D. degree in intelligent mechanical systems engineering with the Graduate School of Engineering, Kagawa University, Takamatsu, Japan.

He has authored over four refereed journal and conference papers. His current research interests include robotic catheter systems for biomedical applications and signal processing.

Shuxiang Guo (Fellow, IEEE) received the Ph.D. degree in mechano-informatics and systems from Nagoya University, Nagoya, Japan, in 1995.

He is currently a Full Professor with the Graduate School of Engineering, Kagawa University, Takamatsu, Japan. He is also a Chair Professor with the Key Laboratory of Convergence Medical Engineering System and Healthcare Technology, Beijing Institute of Technology, Beijing, China. He has authored about 710 refereed journal and conference papers. His current research includes underwater robots, medical robot systems for minimal invasive surgery, micropump, and smart material (SMA, IPMC) based on actuators.

Dr. Guo is an Editor-in-Chief of the *International Journal of Mechatronics and Automation*.

Peng Shi (Student Member, IEEE) received the B.S. degree in mechanical design manufacture and automation from the Huanghe Science and Technology College, Zhengzhou, China, in 2015, and the M.S. degree in control engineering from the Tianjin University of Technology, Tianjin, China, in 2018. He is currently pursuing the Ph.D. degree with Kagawa University, Takamatsu, Japan.

He has authored over six refereed journal articles and conference papers. His current research interests include robotic catheter systems for biomedical applications.

Xiaoliang Jin (Student Member, IEEE) received the B.S. degree in electronic and information engineering from the University of Science and Technology Liaoning, Anshan, China, in 2016, and the M.S. degree in control engineering from the Tianjin University of Technology, Tianjin, China, in 2019. He is currently pursuing the Ph.D. degree with Kagawa University, Takamatsu, Japan.

He has authored over eight refereed journal and conference papers. He researches on robotic catheter systems for biomedical applications.

Masahiko Kawanishi received the B.S. degree from the Faculty of Medicine of Kagawa Medical University, Miki, Japan, in 1993.

He is currently a Lecturer with the Faculty of Medicine, Kagawa University, Takamatsu, Japan. He has authored over 80 refereed journal and conference papers. His current research includes the surgical techniques of neurosurgical operations and intravascular surgery system.

Keisuke Suzuki is currently a Professor with the Graduate School of Engineering, Kagawa University, Takamatsu, Japan. He is one of the research leaders promoting projects on the optimization of human–machine interface for the design of advanced driving support systems. His major research area is human–machine interface of various kinds of traffic mobilities.

Prof. Suzuki is a fellow of JSAE. He is also the Chairman of the Advanced Simulator Study Group organized by JSME.